8th ICATT (International Conference on Astrodynamics Tools and Techniques)
23 - 25 June 2021, Virtual Event, The Netherlands

A MULTI-FIDELITY OPTIMIZATION PROCESS FOR COMPLEX MULTIPLE GRAVITY ASSIST TRAJECTORY DESIGN

Andrea Bellome[(1)], **Joan-Pau Sánchez**[(1)], **Stephen Kemble**[(1)], **Leonard Felicetti**[(1)]

[(1)] *School of Aerospace Transport and Manufacturing, Cranfield University, andrea.bellome@cranfield.ac.uk*

ABSTRACT

Multiple-gravity assist (MGA) trajectories exploit successive close passages with Solar System planets to change spacecraft orbital energy. This allows to explore orbital regions that are demanding to reach otherwise. However, to automatically plan an MGA transfer it is necessary to solve a complex mixed integer programming problem, to find the best sequences among all combinations of encountered planets and dates for the spacecraft manoeuvres. MGA problem is characterized by multiple local minimum solutions and an optimizable parameter space of complex configuration. Current approaches to solve MGA problem require computing time that rise steeply with the number of control parameters, such as the length of the MGA sequence. Moreover, the most useful problem to be solved is a multi-objective optimization (generally with Δv and transfer duration as fitness criteria) since it allows to inform the preliminary mission design with the full extent of launch opportunities. With the present paper, a novel toolbox named ASTRA (Automatic Swing-by TRAjectories) is described to assess the possibility of solving these challenges. ASTRA employs multi-fidelity optimization to construct feasible planetary sequences. It automatically selects planetary encounters and evaluates Lambert's problem solutions over a grid of transfer times. Discontinuities between incoming and outgoing Lambert arcs are in part compensated by the fly-by of the planet. If required, an additional Δv manoeuvre is added, representing the defect between incoming and outgoing spacecraft relative velocity with respect to the planet. Once the solutions are obtained, defects are replaced with Deep Space Manoeuvres (DSMs) between two consecutive encounters. Particle Swarm Optimization (PSO) is used to find the optimal location of DSMs. Mission scenarios towards Jupiter are used as test cases to validate and demonstrate the accuracy of ASTRA solutions.

1 INTRODUCTION

In interplanetary missions, multiple-gravity assist (MGA) manoeuvres make use of successive passages, also called swing-bys or fly-bys, with planets to change the spacecraft heliocentric velocity. This permits to gain or lose energy with no propellant expenditure, thus allowing to explore regions in the Solar System that would be demanding to reach. For example, Galileo [1], Cassini [2], and the more recent BepiColombo [3], Solar Orbiter [4] and JUICE [5] required or will require multiple fly-bys with Venus, Earth and even Jupiter to reach desired scientific orbit.

The design of such missions presents the complication that the trajectory structure, namely planetary sequence, is not known a priori, but is the objective of the optimization itself, leading to a complex mixed-integer non-linear programming (MINLP) problem [6], also known in literature as Hybrid Optimal Control Problem (HOCP) [7]. This is one of the most challenging optimization problems, as

Copyright © The Authors. Published by ICATT. This is the Author Accepted Manuscript. Please refer to any applicable publisher terms of use.

it requires the solution of a combinatorial problem mixed with optimal control theory. MINLP/HOCP can be seen as two coupled optimization problems: the combinatorial part aiming at choosing the optimal sequence of fly-bys, and the continuous part aiming at identifying one or more locally optimal trajectories for a candidate planetary sequence. The MGA problem complexity is due to the fact that these two components are highly coupled, that is the goodness of candidate sequence depends upon the solution of the continuous optimization and a variation of even a single fly-by body corresponds to a significantly different set of trajectories. As such, continuous optimization of the MGA problem is characterized by multiple local minimum solutions and an optimizable parameter space of complex configuration.

The automatic solution of the MGA problem, i.e. finding feasible sequences of planetary encounters and at least one locally optimum trajectory for the given sequence, has been assessed with many different strategies. For example, Chilan and Conway [8], Wall and Conway [9] and Englander, Conway and Williams [10, 11] employed integer genetic algorithm and a real-valued heuristic algorithm for tackling the combinatorial and continuous part, respectively, with both impulsive and low-thrust manoeuvres. Ceriotti and Vasile [12] used a method inspired by ant colony optimization to solve the MGA problem with Deep Space Manoeuvres (DSMs), occuring at the apses of the given planet-to-planet leg. Gad and Abdelkhalik [13, 14] applied a real-valued genetic algorithm using 'hidden genes' and dynamic population size to find flyby sequences and the associated optimal trajectory. Wagner and Wie [15] also employed stochastic genetic algorithm to search the design space, and gradient-based optimization tools to look for locally optimal trajectories. Vasile and De Pascale [16] used evolutionary algorithm with systematic branching approach to optimize the MGA problem. Strange and Longuski [17] developed a method based on Tisserand plot to generate planetary sequences towards a desired planet, employing a simplified circular-coplanar orbital dynamics for Solar System planets.

There is even more extensive literature addressing the continuous optimization of the MGA trajectory design, i.e. the problem of finding local optimal trajectories for a given planetary sequence. For example, Vinkó and Izzo [18] described some global optimization algorithms which could be used in assessing the goodness of a given planetary sequence. Some of them include particle swarm optimization [19], genetic algorithms [13, 14, 18, 20, 21], monotonic basin hopping and ant colony optimization [20], or differential evolution [22]. Approaches based upon systematic scans of the search domain are also available, such as STOUR [23, 24, 25], and GASP [26].

Nonetheless, current approaches to tackle automatic planning of MGA missions often struggle, or fail, to identify global optimum transfers. They tend to employ metaheuristic strategies, such as Genetic Algorithms and Ant Colony Optimization, to scan transfer options, which are not guaranteed to converge to the optimal solution. Moreover, they require a large computing time, that rises with the number of control parameters, such as the length of the sequence or presence of DSMs, and the relationship of which depends upon the type of optimizer employed. Also, they strongly rely on a-priori knowledge of the solutions, such as the departing dates and hyperbolic excess speeds. In addition, current approaches often struggle to obtain true Pareto sets that reflect the multi-objective nature of the problem. Finally, regarding graphical tools such as Tisserand plots [17], even though they can quickly assess the feasibility of different gravity assist sequences, they do not provide explicit information about mission duration or eventual DSM costs [27]. In this way, the combinatorial solution only provides sequences which are energetically possible, but planets synchronicity may only rarely occur.

With the present paper, a quasi-systematic search approach, and its toolbox, to solve automatic MGA problems is presented. The toolbox, referred thereafter as ASTRA (Automatic Swing-by TRAjectories), attempts to solve the issues described above. ASTRA can automatically solve the MGA

problem based upon evaluations of Lambert's problem solutions over grids of departing epochs and transfer times between two successive planets of a given leg of the transfer. Based upon multi-fidelity paradigm [28], ASTRA employs a low-fidelity model on which a specific MGA model is implemented to assess the feasibility of a given route, based upon approximated Δv occurring right at the each swing-by planet, referred as infinity velocity defects. This allows for significant reduction of optimization parameters, while maintaining good representation of actual design space. This permits to obtain wide Pareto sets for missions of interest, approximating any manoeuvres required in the mission. An energy-based criterion is employed to select achievable planets, provided the incoming relative velocity at current fly-by. A higher-fidelity model is then used in conjunction with a Particle Swarm Optimizer (PSO) to refine and obtain of the actual DSMs needed in-between two successive planetary encounters.

2 MULTIPLE GRAVITY ASSIST TRAJECTORY DESIGN

The MGA trajectory design is a global optimization problem in its nature, as for a given trajectory option, namely a planetary sequence, there exist several locally optimal trajectories, in terms of planet phasing, presence of DSMs, etc. Designing an MGA trajectory corresponds to solving a MINLP problem, as it involves the optimization of both integer and continuous variables. A general formulation of a MINLP is provided as in [6, 27], where there is an objective function to be minimized, i.e. $f(x, y)$. Vectors (x, y) include the decision variables of the optimization: the components of x are the continuous variables, while the components of y are the discrete variables.
In an MGA mission design, the discrete components of y correspond to the unknown planetary sequence, while x includes the continuous-varying variables, as the departing date, transfer times between planets, fly-by parameters and so on. The combination of discrete and continuous variables forms a challenging MINLP problem, as a variation of even a single component of y vector requires a considerably different x vector in order to define a new viable transfer. Based upon mission requirements, vector x can be used to define any n-impulse manoeuvre or even continuous acceleration transfer. ASTRA toolbox implements only two- and three-impulse manoeuvres, which as will be discussed, provide a good level of detail for impulsive MGA transfer design. In both cases, a three-dimensional patched conic approach [29] is employed to model the trajectory in the proximity of planetary swing-by. Missions not requiring DSMs during the cruise phase can be tackled with the two-impulses model on which the two impulses correspond to the Lambert's problem solution discontinuities at the planetary encounters. The impulses are then provided by the process of the gravity assist, i.e. the spacecraft velocity vector deflection. This is the case, for example, of JUICE mission to Jupiter [5]. In this case, the x vector only contains the departing date and transfer times between two successive planets. However, there are cases on which the spacecraft requires large DSMs, in the order of hundreds of meters per second, on its way to the target planet to shorten the time of flight. This is the case of Cassini transfer towards Saturn [2]. In the latter, a three-impulses model should be employed to design transfers for each leg of the MGA sequence. This is known in literature as the MGA-DSM model [16, 18] on which the interplanetary planet-to-planet leg is propagated until a fraction of the transfer time before performing a midcourse DSM. In this case, vector x contains four variables for each of the gravity-assist planets [16, 27], that are the time of flight between two successive planetary encounters, flyby altitudes, hyperbola plane inclination and presence of DSM.
For the purpose of the present paper, both two-impulses and three-impulses models are useful as: 1) two-impulses approach can represent interplanetary legs with manoeuvres applied right after the fly-by of the departing planet for that leg, i.e. the infinity velocity defects. This well approximates transfers where small correction DSMs, in the order of tens of meters per second, are employed;

2) MGA-DSM model is used as post-processing step. The MGA-DSM is particularly necessary to model and refine interplanetary legs with large discontinuities arising from the two-impulses model.

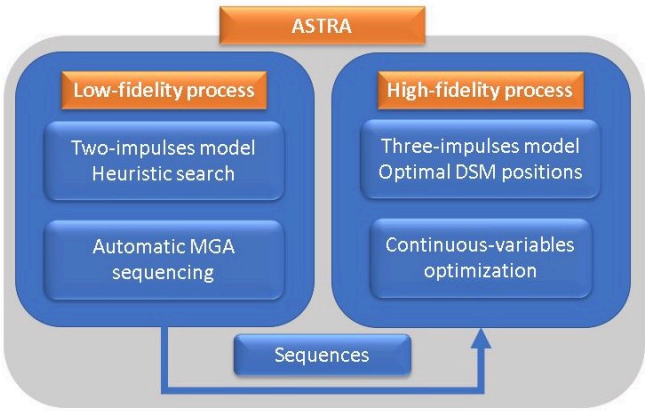

Figure 1: ASTRA multi-fidelity approach to MGA mission design.

Figure 1 shows how the two models, associated to different fidelities, are employed in ASTRA main engine. In the low-fidelity process, ASTRA employs the two-impulses model coupled with heuristic strategies (see also later section 3.1.1) to automatically construct MGA sequences. Then, in the high-fidelity block, ASTRA post-processes the obtained results via direct optimization of solutions coming from the low-fidelity block, by optimally replacing the defects with mid-course DSMs in between two successive planetary encounters. A further option in utilisation of multi-fidelity methods is the use of simplifications in the mathematical models of planetary motion in the first of the two stage optimisation processes, such as circular co-planar orbits. This option can potentially lead to efficient problem solutions because of the inherent simplifications that the first approximation may allow. A potential difficulty arises from the transition to Process 2 where a non-coplanar planetary model is used to generate real world transfers. In this second model, planetary velocity components can vary significantly from the circular case. This difficulty is avoided here by using the same planetary model in both processes.

2.1 Two-impulses model

The lower-fidelity MGA transfer description is based upon successive Lambert arcs connecting two consecutive swing-bys, e.g. in STOUR [23, 24, 25]. The cost of an MGA leg (without midcourse DSMs) could be either approximated by a powered fly-by or by a small manoeuvre applied after the first planet of the leg. A powered fly-by model assumes a Δv manoeuvre at the pericentre of the incoming swing-by hyperbola to match the incoming and outgoing spacecraft velocities. However, this method has not been implemented in the context of real interplanetary missions, due to navigation challenges that it arises. Therefore, Δv on each leg of the MGA sequence are computed as defects between incoming and outgoing spacecraft relative velocity with respect to the planet, which are solutions of Lambert's problem for the given leg. These velocity discontinuities between legs are thus considered as impulsive manoeuvres applied right after the planetary encounter.
The change of direction between incoming and outgoing legs of the fly-by is computed through the angle δ, such that $cos(\delta) = \frac{\vec{v}_\infty^- \cdot \vec{v}_\infty^+}{|\vec{v}_\infty^-||\vec{v}_\infty^+|}$, where $\vec{v}_\infty^-$ and $\vec{v}_\infty^+$ are the spacecraft relative velocity with respect to the flyby planet (also called infinity velocities). Superscripts $-$ and $+$ are used to describe incoming and outgoing variables, respectively. Angle δ is then found from the inverse cosine with a positive

180-degree range. The maximum deflection is limited by the periapsis of the fly-by hyperbola r_p through: $\delta_{max} = 2asin([1 + \frac{r_{p,min}|\vec{v}_\infty^-|^2}{\mu_{pl}}]^{-1})$, where $r_{p,min}$ is the the minimum allowable periapsis and μ_{pl} is the gravitational parameter of the fly-by planet (see also section 3.2). Discontinuities between $\vec{v}_\infty^-$ and $\vec{v}_\infty^+$, which we call infinity velocity defects, are then compensated through a Δv computed immediately after the fly-by [30]:

$$\Delta v = \begin{cases} ||\vec{v}_\infty^+| - |\vec{v}_\infty^-||, & \text{if } \delta \leq \delta_{max} \\ \sqrt{|\vec{v}_\infty^+|^2 + |\vec{v}_\infty^-|^2 - |\vec{v}_\infty^+||\vec{v}_\infty^-| \cos(\delta_{max} - \delta)}, & \text{otherwise} \end{cases}$$

Note that since $\vec{v}_\infty^-$ and $\vec{v}_\infty^+$ represent spacecraft velocities relative to the fly-by body, the Δv ultimately depends upon planet ephemerides, through its heliocentric velocity at the encounter epoch. Therefore, vector x, in its low-fidelity representation, only contains the departing epoch t_0 and the time of flight (TOF) for all the legs (i.e. $x = [t_0, TOF_1, ..., TOF_{n-1}]$, where n is the number of planets in the sequence). The cost $f(x, y)$ is then typically written as:

$$f(x, y) = |\vec{v}_{\infty,dep}| + \sum_{i=1}^{n-2} \Delta v_i + |\vec{v}_{\infty,arr}| \tag{1}$$

where $\vec{v}_{\infty,dep}$ and $\vec{v}_{\infty,arr}$ are the infinity velocities relative to the departing and arrival planet of the entire MGA sequence, respectively (no Δv is assumed on the first leg of the transfer).

2.2 Three-impulses model

The three impulses model, also called MGA-DSM model, is a well-known approach to tackle optimization of MGA transfers [16, 18] with regards to continuous-varying variables contained in x vector. In the MGA-DSM model, an impulsive manoeuvre is used to replace the infinity velocity defect at the first planetary encounter of a given leg. The DSM is computed as a velocity discontinuity applied after a fraction k of the time of flight TOF of a given leg. The next planet is then targeted with a solution of Lambert's problem and the DSMs is derived. Therefore, each flyby is now characterized by $|\vec{v}_\infty^-| = |\vec{v}_\infty^+|$ where:

$$\vec{v}_\infty^+ = \vec{v}_\infty^-[\cos\delta\hat{b}_1 + \sin\zeta\sin\delta\hat{b}_2 + \cos\zeta\sin\delta\hat{b}_3] \tag{2}$$

on which: δ is the deflection angle, ζ describes the rotation of the relative velocity through the inclination of the fly-by hyperbola in planetary reference frame. Vectors $\hat{b}_1$, $\hat{b}_2$ and $\hat{b}_3$ are the b-plane unit vectors and are defined as: $\hat{b}_1 = \vec{v}_\infty^-/|\vec{v}_\infty^-|$, $\hat{b}_2 = (\hat{b}_1 \times \vec{r}_i)/|\vec{r}_i|$ ($\vec{r}_i$ being the position vector of the fly-by planet), and $\hat{b}_3 = \hat{b}_2 \times \hat{b}_1$ (see also [31]). Thus, the number of decision variables is increased by three (i.e. r_p, k and ζ) for each planetary encounter, compared to the two-impulses model.

3 BUILDING THE ROUTE SET IN ASTRA

ASTRA employs a multi-fidelity approach to automatically solving the MGA problem. The pipeline consists in two successive processes (see also Figure 1): 1) Process 1: Automatic MGA sequence construction; 2) Process 2: Route refinement and post-processing.
The low-fidelity Process 1 allows to generate a list of successive possible encounters with Solar System planets, by means of energetic considerations at current planetary swing-by. Transfer options towards identified planets are then evaluated by successively solving Lambert's problem over a grid of arrival dates at next planet encounter. A two-impulses model as described in section 2.1 is used to compute the Δv defects. This process is repeated until the target planet is reached. In the higher-fidelity Process 2, ASTRA orders all the routes constructed in previous steps according to a ranking criterion, which typically is the cost expressed in equation 1, or the total transfer time, or a combination thereof. Moreover, fly-by parameters (r_p, ζ) are obtained for all the swing-bys in the sequences, and ultimately the Δv defects are replaced by mid-course DSMs between two successive planetary encounters via refinement optimization using the MGA-DSM model described in section 2.2.

3.1 Process 1: Automatic MGA sequence construction

Algorithm 1 Building the route set in ASTRA's Process 1 with two-impulses low-fidelity model.

```
1:  Select departing and target planets and departing date range
2:  for each departing date do
3:      while the target planet is not reached do
4:          check the achievable planets
5:          for each planet identified do
6:              Lambert arc transfer exploration for the range of feasible transfer times
7:              compute the defects
8:          end
9:          apply filtering criteria                          ▷ see section 3.1.1
10:     end while
11: end
```

Algorithm 1 illustrates the main systematic search process implemented in ASTRA's low-fidelity Process 1. The process requires first to identify the departure and target (final) planet, as well as the discretised launch window (i.e.,vector of start or departure dates). At the start of each successive leg (i.e., line 4 in Algorithm 1), a swing-by assessment step is needed to generate the list of successive reachable planets. Thus, the outgoing relative velocity vectors that maximises and minimises the energy of the spacecraft at departure of the current planet are calculated and used to assessed the planets that can be crossed and, so, potentially reached. Figure 2 depicts this process for all legs, other than the departure leg, where the outgoing relative velocity at the departing planet $|\vec{v}_{\infty,dep}|$ can be defined instead by the launcher capability.
Figure 2 assumed that incoming relative velocity $\vec{v}_\infty^-$ is deflected by the angle δ such that the closest possible alignment with the gravity-assist body velocity $\vec{v}_{ga}$ is achieved post swing-by. If minimum pericentre allows the relative velocity vector post swing-by $\vec{v}_\infty^+$ would become aligned with $-\vec{v}_{ga}$ or $\vec{v}_{ga}$, i.e. minimizing or maximizing energy. Therefore, after the swing-by, the spacecraft heliocentric velocity $\vec{v}_{sc}^+$ would be $\vec{v}_{sc}^+ = -|\vec{v}_\infty^-|\vec{v}_{ga}/|\vec{v}_{ga}|$ or $\vec{v}_{sc}^+ = |\vec{v}_\infty^-|\vec{v}_{ga}/|\vec{v}_{ga}|$ only if $\alpha + \delta_{max} \geq 180^o$ (in-front passage), or $\alpha - \delta_{max} \leq 0^o$ (behind passage), respectively (see Figure 2). The angle α (positive in 180-degree range) can be computed from geometry from Figure 2 as $\alpha = acos(\frac{\vec{v}_\infty^- \cdot \vec{v}_{ga}}{|\vec{v}_\infty^-||\vec{v}_{ga}|})$.

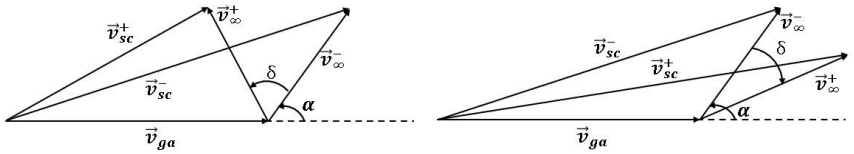

Figure 2: Heliocentric velocity change due to swing-by in front of the planet (left image), and behind the planet (right image). Left and right cases result in minimizing and maximizing the energy after the swing-by, respectively. The angle α is a geometry parameter used to describe minimum/maximum energy post swing-by.

However, if the condition $\alpha + \delta_{max} \geq 180^o$ and/or $\alpha - \delta_{max} \leq 0^o$ are not satisfied, one looks for the closest possible alignment of $\vec{v}_{\infty}^{+}$ with $\vec{v}_{ga}$ by computing $\vec{v}_{\infty}^{+}$ as in equation 2, with $\delta = \delta_{max}$, for both $\zeta = 90^o$ (in-front passage) and $\zeta = 270^o$ (behind passage). This procedure allows estimation of maximum apocentre/pericentre achievable post swing-by, and hence the reachable planets.
Once the list of reachable planets has been computed, the next step consists in evaluating the transfer options for each of the targets identified. A grid of transfer times between the two planets in the specified leg is used to solve the Lambert's problem. The number of revolutions considered for the Lambert solver must also be specified. The range of transfer duration considered per leg mainly depends on the planets considered and the number of revolutions specified for the Lambert solver (see 4.1 for further details).
Each solved planet-to-planet arc allows defining a Δv penalty or cost, associated with the departure planet of the specific leg, which becomes the basis for the enumerative search algorithm applied in Process 1. Figure 3 illustrates the tree structure of the search space as defined by Algorithm 1. At the very first departure planet of the MGA sequence (i.e. the Earth), this Δv penalty is simply defined as the excess velocity at departure $|\vec{v}_{\infty,dep}|$. However, for any subsequent leg, equations from section 2.1, yield the Δv costs associated with the velocity discontinuity between the incoming and outgoing asymptotes of the departure planet in the planet-to-planet Lambert arc. These Δv costs, referred thereafter as Δv defects, are stored for each route considered and used as the heuristic information to inform the filtering criteria described in 3.1.1. Algorithm 1 is thus iterated until a stopping criterion is met (e.g. if target planet is reached) and the outputted route set can be fed to Process 2 for post-processing and refinement.

3.1.1 Filtering and heuristic information

As algorithm 1 is iterated, the number of identified routes stored and sorted grows. If particularly long fly-by sequences are sought, the number of possible routes may potentially grow to unmanageable numbers. However, this problem is mitigated via the application of both an incremental pruning and Beam Search strategy to identify and filter out infeasible routes. Both of these filters are based on heuristic information that can be directly related with practical mission design constraints: 1) infinity velocity at the departing planet, i.e. $|\vec{v}_{\infty,dep}|$, 2) size of Δv defect applied at each fly-by, 3) Infinity velocity at arrival, $|\vec{v}_{\infty,arr}|$. An upper limit for these three parameters ($|\vec{v}_{\infty,dep}|$, Δv defects, $|\vec{v}_{\infty,arr}|$) can be identified and used in a process of incremental pruning [32] for each planet-to-planet batch of Lambert arc solutions. Assuming the Earth as the nominal departing planet, an upper limit on $|\vec{v}_{\infty,dep}|$ can be identified from current launcher performances. On the other hand, constraints on $|\vec{v}_{\infty,arr}|$ depend upon spacecraft performance considerations, as it is linked with the propellant required to

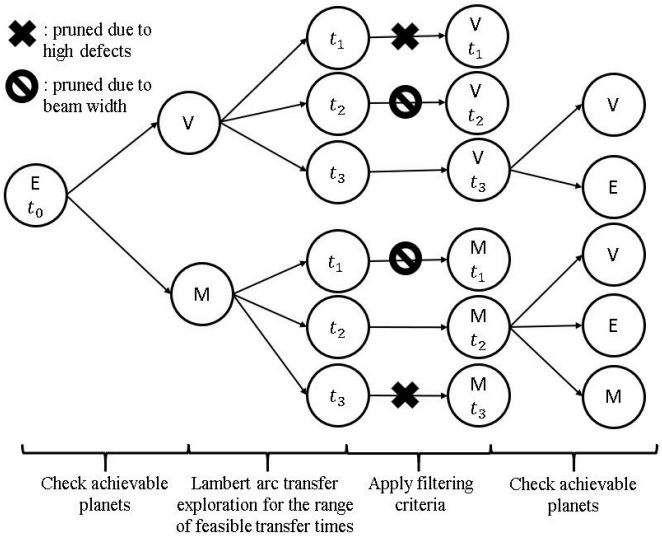

Figure 3: Tree expansion for automatic MGA solution as done by ASTRA's Process 1. 'E', 'V' and 'M' stand for Earth, Venus and Mars, respectively, while t_i with $i = 0, 1, ...$ refers to epoch at which the planet is visited. Reference to planets and dates are given for example purposes only.

inject the spacecraft around the desired planet. For the purpose of the present paper, filter values that are applied are $|\vec{v}_{\infty,dep}| < 6\ km/s$ and $|\vec{v}_{\infty,arr}| < 8\ km/s$.
Regarding constraints over Δv defects at each swing-by, these are linked to limitations on spacecraft propulsive system, thus large values are not feasible for standard spacecraft designs. To achieve computational efficiency, Δv defects should be the minimum possible, but subject to the condition that locally optimal solutions are not lost and the Pareto sets characteristics are retained. This implies an upper limit on the DSM in-between two consecutive swing-bys, which is related by the leveraging ratio (i.e. ratio between Δv defect and precedent DSM). The leveraging ratio varies between typically 0.5 and 6.5 for the range of missions considered in the present paper; so for example a maximum defect of $2000\ m/s$ implies a maximum DSM magnitude of about $310\ m/s$ in the extreme leveraging cases (note that 6.5 is still a high leveraging ratio and will be generally less than this). Therefore, in this paper, only $\Delta v \leq 2000\ m/s$ are retained for further considerations.
While in first instance these upper limits are used to filter out all the branches that do not satisfy these criteria, the number of stored routes can still grow to unmanageable numbers. Thus, a simple Beam Search (BS) strategy [33, 34] is also implemented, on which non-promising solutions under construction are discarded. The size of the beam, designated as the beam width, governs the selection process, as it represents the number of options retained for successive expansion. A full grid search, on which the beam width is the maximum allowed, carries forward all solutions observing the defect limits. This ultimately has computer memory implications. For the purpose of the present paper, a wide beam can carry forward more solutions with larger defects, for consideration in the final Pareto set after the arrival at the target. On the other hand, a too narrow width will prune out local optima solutions. A good compromise for beam width between computational efficiency and Pareto sets completeness has been found to be between 3 to 60.

3.2 Process 2: routes refinement and post-processing

The set of routes obtained from Process 1 is sorted to find the minimum objective function value as expressed in equation 1. A non-dominant Pareto front of mission overall duration and objective value

can then be derived. Pareto fronts are computed based on the Δv defects as computed in equations from section 2.1. However, Δv defects are manoeuvres applied immediately after departure from a fly-by and so they do not represent real manoeuvres in the context of a mission design. Therefore in ASTRA, as a post-processing stage, after results are obtained and sorted, these Δv defects are converted to DSMs between two successive planets in the sequence. This is done employing the MGA-DSM three-impulses model described in section 2.2.
As first step of post-processing stage, fly-by parameters r_p and ζ need to be derived. For each swing-by encounter, Process 1 has provided $\vec{v}_\infty^-$ and $\vec{v}_\infty^+$, as well as the encounter epochs. Therefore, similarly as already done in section 2.1, one computes if the Δv defect can be compensated with the gravity of the current fly-by body or not, checking if $\delta \leq \delta_{max}$. If the condition is satisfied, then an r_p exists such that the infinity velocity post fly-by is $|\vec{v}_\infty^-|\vec{v}_\infty^+/|\vec{v}_\infty^+|$. In this case, the eccentricity e and semi-major axis a of the fly-by hyperbola are: $e = [\sin\frac{\delta}{2}]^{-1}$ and $a = -\frac{\mu_{pl}}{|\vec{v}_\infty^-|^2}$. Where μ_{pl} is the gravitational parameter of the fly-by body. Therefore, the periapsis radius is: $r_p = a(1-e)$. However, if the condition $\delta \leq \delta_{max}$ is not satisfied, one assumes the maximum deflection fly-by defined by $r_p = r_{p,min}$. For the purposes of the present paper, a minimum altitude of 200 km is considered for Venus, Earth and Mars fly-bys. Once r_p and thus δ are known, one can compute the fly-by angle ζ by inverting equation 2. One computes the vector $\vec{w} = [w_1, w_2, w_3]^T = [\cos\delta, \sin\zeta\sin\delta, \cos\zeta\sin\delta]^T$ as $\vec{w} = \frac{1}{|\vec{v}_\infty^+|}M^{-1}\vec{v}_\infty^+$. Where the matrix $M = [\hat{b}_1, \hat{b}_2, \hat{b}_3]$ is found from the definition of $\hat{b}_1$, $\hat{b}_2$ and $\hat{b}_3$ as described in section 2.2. Finally, one has $\zeta = \arctan(w_2/w_3)$, positive in the 360-degrees range.
As second step of post-processing stage, the Δv defects need to be replaced with DSMs occurring after a fraction of the transfer time between two consecutive swing-bys, according to the MGA-DSM model provided in section 2.2. ASTRA employs Particle Swarm Optimization (PSO) [35], [36] to look for the optimal location of DSM along the given leg of the transfer. The optimiser is initialised using solutions from Process 1, and derived fly-by parameters and time intervals are used to derive control inputs for the full optimiser. Such an optimization efficiently converges to the solution (see 4.1), eliminating defects and inserting DSMs where optimal.

4 CASE STUDIES

Optimal transfers are determined for benchmark missions to test the performances of ASTRA solver. An MGA mission towards Jupiter is tested referring to European Space Agency (ESA)'s JUICE mission [5], due to launch in 2022. JUICE is intended to follow the sequence Earth-Earth-Venus-Earth-Mars-Earth-Jupiter (the first planet being the departing one).

4.1 Missions towards Jupiter

Transfers towards Jupiter are explored for a departure date in 2023. This allows to benchmark ASTRA solutions with those proposed by the ESA's mission JUICE [5]. Note that JUICE departure from Earth is set in 2022 and its first gravity assisted manoeuvre is also at Earth in May 2023. The spacecraft will then encounter Venus, Earth, Mars, and Earth again to increase its energy, resulting in an EEVEMEJ sequence ('E', 'V', 'M' and 'J' stand for 'Earth', 'Venus', 'Mars' and 'Jupiter', respectively). However, the first leg of the mission is a one-year Earth resonant transfer whose main function is to allow a plane change at the Earth fly-by to swing the orbit plane close to the ecliptic. ASTRA, as a preliminary trajectory design tool, does not implement considerations on the available declinations of the Earth departure asymptote. Therefore, in order to appropriately benchmark the published trajectories for JUICE mission, a departure in 2023 is considered instead. The full 2023 launch window is explored, with departing dates separated by steps of 10 days.

Table 1: Results for JUICE trajectory compared to ASTRA solutions in 2023 launch window. If a Δv is not present on a given leg, a "−−" is included in the table.

Event	**Actual JUICE**	**ASTRA (Process 1)**	**ASTRA (Process 2)**
Launch	28/05/2023	20/05/2023	20/05/2023
C_3	10.1 km^2/s^2	10.9 km^2/s^2	10.0 km^2/s^2
Venus	21/10/2023	19/10/2023	18/10/2023
Δv_1	−−	72 m/s	−−
Earth	31/08/2024	01/09/2024	31/08/2024
Δv_2	−−	17 m/s	−−
Mars	11/02/2025	10/02/2025	10/02/2025
Δv_3	−−	18 m/s	−−
Earth	24/11/2026	26/11/2026	25/11/2026
Δv_4	−−	−−	−−
Jupiter	07/10/2029	19/10/2029	11/11/2029
C_3	30.7 km^2/s^2	30.9 km^2/s^2	31.0 km^2/s^2

The maximum number of encountered planets, not accounting for the departing and arrival ones, has been limited to five, leading to a maximum length of seven planets in the whole sequence. This is because a larger number would excessively increase the transfer time while adding little benefits. For this test case, a beam width of 3 is used, meaning that each time a planet is added to a given route, the best three transfer options are retained for further expansion when at transfer times grid evaluation in Process 1. This is enough for ASTRA's Process 1 to capture primary missions of interest with reduced defects.

Table 2: Results for ESA's EVEEJ trajectory with 2:1 resonance on the EE leg, compared to ASTRA solutions in 2023 launch window. If a Δv is not present on a given leg, a "−−" is included in the table.

Event	**ESA's EVEEJ**	**ASTRA (Process 1)**	**ASTRA (Process 2)**
Launch	03/06/2023	02/06/2023	02/06/2023
C_3	9.31 km^2/s^2	10.9 km^2/s^2	10.9 km^2/s^2
Venus	25/11/2023	25/11/2023	25/11/2023
Δv_1	−−	13 m/s	−−
Earth	22/10/2024	22/10/2024	22/10/2024
Δv_2	−−	−−	−−
Earth	22/10/2026	22/10/2026	22/10/2023
Δv_3	−−	−−	−−
Jupiter	20/01/2030	20/01/2030	20/01/2030
C_3	31.2 km^2/s^2	31.1 km^2/s^2	31.1 km^2/s^2

In order to map the full range of revolutions between each planet, successive runs are needed. For the purposes of the present paper, a reduced set of running options has been employed, meaning that maximum one leg in the sequence is allowed to have more than one revolution (up until to two revolutions). This is because every full revolution implies more than one additional year of transfer

time, thus increasing the total time of flight considerably. Moreover, the main aim of ASTRA is to assess the feasibility of finding promising encounters. However, this reduction of transfer options still allows to identify primary missions of interest for the Jupiter case.

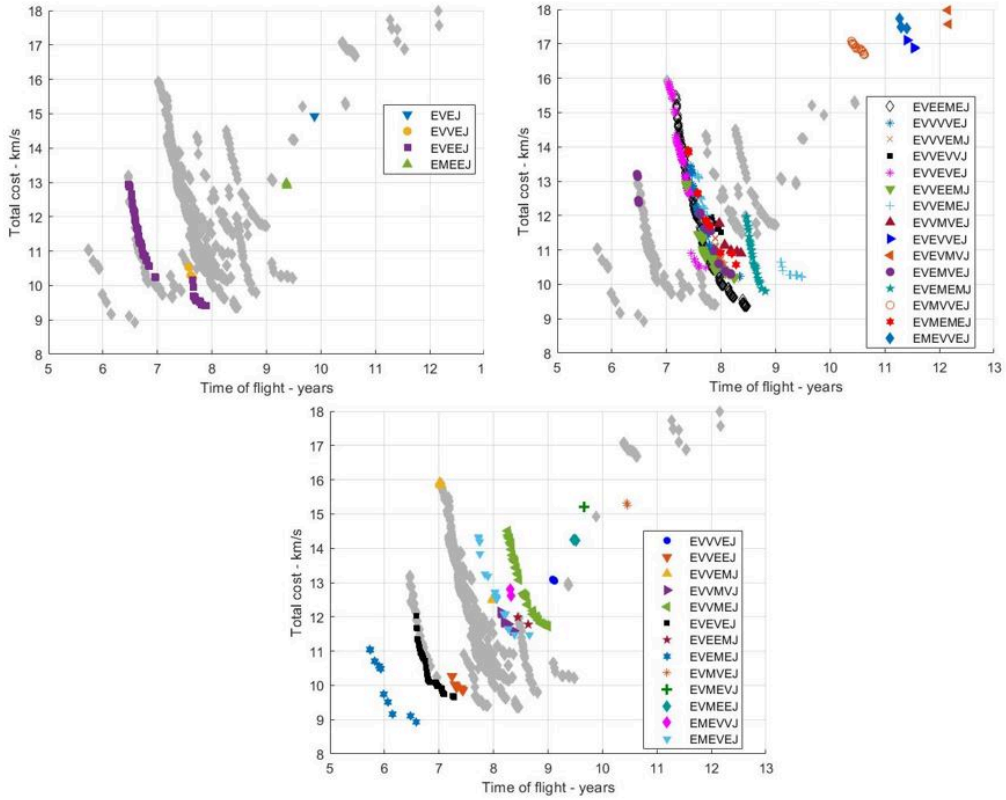

Figure 4: Pareto fronts for sequences towards Jupiter for departure date in 2023 as resulting from Process 1. Total cost refers to objective function as in equation 1. Top-left image highlights sequences with four and five planets, top-right image highlights sequences with six planets, and bottom image highlights sequences with seven planets.

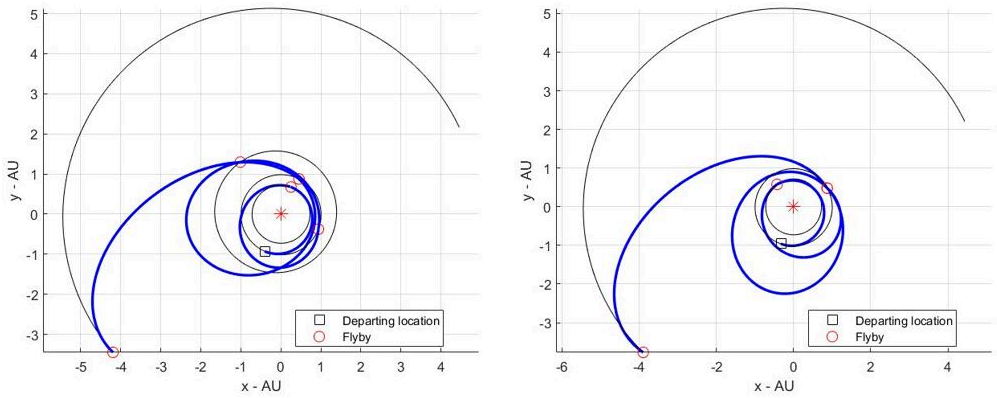

Figure 5: JUICE-like EVEMEJ (left) and EVEEJ (right) transfers with departure date in 2023, obtained from ASTRA's Process 1. From innermost to outermost, black circles represent Venus, Earth, Mars and Jupiter orbits, respectively.

Pareto sets of available transfer opportunities as resulting from Process 1 of ASTRA search are shown in Figure 4. As expected, among the sequences, the EVEMEJ is found to be the optimal one, i.e. the one with lowest total cost and transfer time. Note that also the well-known sequence EVEEJ performs well in 2023 launch window, provided the 2:1 resonance between the consecutive Earth swing-bys (note that resonant transfers are computed separately from main search engine as in Algorithm 1 and following the procedure found in [15]). Details of EVEMEJ and EVEEJ sequences, compared to actual JUICE [37] and ESA Red Book [1], are provided in Table 1 and 2. Figure 5 show ecliptic projection of EVEMEJ and EVEEJ transfers. Alternative interesting options towards Jupiter for a launch in 2023, as resulting from ASTRA's Process 1 and 2, are reported in Tables 3 and 4. Among those, the well-known EVEEJ (without resonance on the EE leg) and EVVEJ are found by ASTRA Process 1, but results indicate both increased transfer duration and higher objective value than previous cases. Another interesting option is the EVEVEJ, since it allows for reduced transfer times, but at the price of higher C_3 at Jupiter.

Table 3: Interesting alternative transfer options towards Jupiter in the 2023 time-frame as resulting from ASTRA's Process 1.

Sequence	**Departing date**	**Departing C_3**	**Δv defects**	**Arrival C_3**	**Transfer time**
EVEVEJ	25/06/2023	14.0 km^2/s^2	740 m/s	44.5 km^2/s^2	6.6 years
EVVEEJ	30/06/2023	14.1 km^2/s^2	430 m/s	33.4 km^2/s^2	7.52 years
EVVEJ	30/06/2023	14.3 km^2/s^2	415 m/s	35.8 km^2/s^2	7.63 years
EVEEJ	26/04/2023	14.3 km^2/s^2	196 m/s	32.0 km^2/s^2	7.76 years
EVVEVEJ	30/06/2023	14.4 km^2/s^2	386 m/s	40.3 km^2/s^2	7.84 years
EVEMVEJ	01/04/2023	11.9 km^2/s^2	1603 m/s	41.9 km^2/s^2	8.25 years

Table 4: Optimized solutions for alternative transfer options towards Jupiter in the 2023 time-frame as resulting from ASTRA's Process 2.

Sequence	**Departing date**	**Departing C_3**	**Δv DSMs**	**Arrival C_3**	**Transfer time**
EVEVEJ	15/06/2023	12.9 km^2/s^2	75.5 m/s	40.4 km^2/s^2	6.74 years
EVVEEJ	18/06/2023	14.4 km^2/s^2	301 m/s	33.52 km^2/s^2	7.54 years
EVVEJ	16/06/2023	14.9 km^2/s^2	389 m/s	34.7 km^2/s^2	7.56 years
EVEEJ	26/04/2023	13.5 km^2/s^2	$--$	32.7 km^2/s^2	7.84 years
EVVEVEJ	18/06/2023	13.4 km^2/s^2	59.4 m/s	41.8 km^2/s^2	7.98 years
EVEMVEJ	08/04/2023	14.1 km^2/s^2	783 m/s	47.3 km^2/s^2	7.99 years

ASTRA, in MATLAB environment, requires 1-5 minutes per departing date on a 2.8 GHz Intel Core i7 to construct solutions with a fixed number of revolutions per leg. Total computing time of about 3-7 hours to map the entire launch window is needed. Despite the seemingly large time, this is consistent with available literature. Current approaches can take from 2 to 3.5 hours to run with simple set ups, i.e. with maximum one revolution for all the legs, usually requiring a priori knowledge on solution. Moreover, they often employ metaheuristic strategies such as Genetic Algorithms of Ant Colony Optimization to scan transfer options, which are not guaranteed to converge to optimal solution, while ASTRA process ensure a systematic exploration of all sequences and opportunities.

[1] https://sci.esa.int/web/juice/-/54994-juice-definition-study-report, last accessed March 10, 2021

5 CONCLUSIONS

This paper presents an efficient approach to solve on a quasi-systematic manner the automatic MGA problem. The search is systematic as in the sense that is performed for all possible combinations of planet-to-planet transfers and for a thick grid of departure conditions and time of flights for all legs. Such an approach is made possible through a multi-fidelity model of the planet-to-planet transfer, on which on its low-fidelity set up is modelled as a planet-to-planet Lambert arc, where all velocity discontinuities are considered as Δv penalties on the fitness function.
Yet, the complete exploration of all possible combination of planet-to-planet transfers and all possible combination of departure and arrival times would be a rather inefficient and computationally cumbersome task. Thus, a filtering process is used for every planet-to-planet combination in order to limit the growth of solutions to only reasonably feasible transfers. This method has proven to be efficient and effective in identifying primary sequences of interest for Jupiter and Saturn mission cases, by performing grid scans of possible planetary encounters and employing a reduced set of control parameters, maintaining good representation of the search space.
Compared to existing approaches, while employing similar computational efforts, ASTRA does not need a priori knowledge of the solution (e.g. on the departing date or velocity) and it is comprehensive in that it automatically considers all feasible planetary fly-by sequences. Moreover, by approximating the DSMs as infinity velocity defects at each planetary encounter, ASTRA is able to generate wide sets of solutions to represent broad Pareto sets useful for preliminary mission analysis.
The key aspect of this approach is therefore the specific multi-fidelity process used, in considering two- and three-impulse transfers and the inclusion of all feasible planet fly-by sequences in any given transfer problem. The transition between processes here is facilitated by the use of the general eccentric 3D planetary motions in both processes of the optimisation.
Future releases of ASTRA will include grid search approach hybridized with tree-like metaheuristic strategies, such as Ant Colony Optimization (ACO), to increase computational efficiency, without scarifying the convergence to global optima solutions. Moreover, future research will also focus on mapping the swing-by discontinuities (i.e. Δv defects) into actual Deep Space Manoeuvres (DSMs) while in the search steps, maintaining efficient computational efforts.

REFERENCES

[1] L. A. D'Amario, D. V. Byrnes, J. R. Johannesen, and B. G. Nolan, "Galileo 1989 VEEGA trajectory design," *Journal of the Astronautical Sciences*, vol. 37, pp. 281–306, 1989.

[2] F. Peralta and S. Flanagan, "Cassini interplanetary trajectory design," *Control Engineering Practice*, vol. 3, no. 11, pp. 1603–1610, 1995.

[3] D. G. Yárnoz, R. Jehn, and M. Croon, "Interplanetary navigation along the low-thrust trajectory of bepicolombo," *Acta Astronautica*, vol. 59, no. 1-5, pp. 284–293, 2006.

[4] J. Sanchez Perez, W. Martens, and G. Varga, "Solar orbiter 2020 february mission profile," *Advances in the Astronautical Sciences*, vol. 167, p. 1395–1410, 2018.

[5] O. Grasset, M. K. Dougherty, A. Coustenis, E. J. Bunce, C. Erd, D. Titov, M. Blanc, A. Coates, P. Drossart, and L. N. Fletcher, "JUpiter ICy moons Explorer (JUICE): An ESA mission to orbit Ganymede and to characterise the Jupiter system," *Planetary and Space Science*, vol. 78, pp. 1–21, 2013.

[6] M. Schlueter, S. O. Erb, M. Gerdts, S. Kemble, and J.-J. Rückmann, "Midaco on minlp space applications," *Advances in Space Research*, vol. 51, no. 7, pp. 1116–1131, 2013.

[7] I. M. Ross and C. N. D'Souza, "Hybrid optimal control framework for mission planning," *Journal of Guidance, Control, and Dynamics*, vol. 28, no. 4, pp. 686–697, 2005.

[8] C. M. Chilan and B. A. Conway, "A space mission automaton using hybrid optimal control," in *17th Annual Space Flight Mechanics Meeting*, 2007, pp. 259–276.

[9] B. J. Wall and B. A. Conway, "Genetic algorithms applied to the solution of hybrid optimal control problems in astrodynamics," *Journal of Global Optimization*, vol. 44, no. 4, p. 493, 2009.

[10] J. A. Englander, B. A. Conway, and T. Williams, "Automated mission planning via evolutionary algorithms," *Journal of Guidance, Control, and Dynamics*, vol. 35, no. 6, pp. 1878–1887, 2012.

[11] J. Englander, B. Conway, and T. Williams, "Automated interplanetary trajectory planning," in *AIAA/AAS Astrodynamics Specialist Conference*, 2012, p. 4517.

[12] M. Ceriotti and M. Vasile, "MGA trajectory planning with an ACO-inspired algorithm," *Acta Astronautica*, vol. 67, no. 9-10, pp. 1202–1217, 2010.

[13] A. Gad and O. Abdelkhalik, "Hidden genes genetic algorithm for multi-gravity-assist trajectories optimization," *Journal of Spacecraft and Rockets*, vol. 48, no. 4, pp. 629–641, 2011.

[14] O. Abdelkhalik and A. Gad, "Dynamic-size multiple populations genetic algorithm for multigravity-assist trajectory optimization," *Journal of Guidance, Control, and Dynamics*, vol. 35, no. 2, pp. 520–529, 2012.

[15] S. Wagner and B. Wie, "Hybrid algorithm for multiple gravity-assist and impulsive delta-V maneuvers," *Journal of Guidance, Control, and Dynamics*, vol. 38, no. 11, pp. 2096–2107, 2015.

[16] M. Vasile and P. De Pascale, "Preliminary design of multiple gravity-assist trajectories," *Journal of Spacecraft and Rockets*, vol. 43, no. 4, pp. 794–805, 2006.

[17] N. Strange and J. Longuski, "Graphical method for gravity-assist trajectory design," *J. Spacecr. Rockets*, vol. 37, p. 9–16, 2002.

[18] T. Vinkó and D. Izzo, "Global optimisation heuristics and test problems for preliminary spacecraft trajectory design," *Advanced Concepts Team, ESATR ACT-TNT-MAD-GOHTPPSTD, Sept*, 2008.

[19] M. Pontani and B. A. Conway, "Particle swarm optimization applied to space trajectories," *Journal of Guidance, Control, and Dynamics*, vol. 33, no. 5, pp. 1429–1441, 2010.

[20] M. Vasile, E. Minisci, and M. Locatelli, "Analysis of some global optimization algorithms for space trajectory design," *Journal of Spacecraft and Rockets*, vol. 47, no. 2, pp. 334–344, 2010.

[21] M. Schlueter, "Nonlinear mixed integer based optimization technique for space applications," 2012.

[22] A. D. Olds, C. A. Kluever, and M. L. Cupples, "Interplanetary mission design using differential evolution," *Journal of Spacecraft and Rockets*, vol. 44, no. 5, pp. 1060–1070, 2007.

[23] J. M. Longuski and S. N. Williams, "Automated design of gravity-assist trajectories to mars and the outer planets," *Celestial Mechanics and Dynamical Astronomy*, vol. 52, no. 3, pp. 207–220, 1991.

[24] J. A. Sims, A. J. Staugler, and J. M. Longuski, "Trajectory options to pluto via gravity assists from venus, mars, and jupiter," *Journal of Spacecraft and Rockets*, vol. 34, no. 3, pp. 347–353, 1997.

[25] A. E. Petropoulos, J. M. Longuski, and E. P. Bonfiglio, "Trajectories to jupiter via gravity assists from venus, earth, and mars," *Journal of Spacecraft and Rockets*, vol. 37, no. 6, pp. 776–783, 2000.

[26] D. Izzo, V. M. Becerra, D. R. Myatt, S. J. Nasuto, and J. M. Bishop, "Search space pruning and global optimisation of multiple gravity assist spacecraft trajectories," *Journal of Global Optimization*, vol. 38, no. 2, pp. 283–296, 2007.

[27] A. Bellome, J.-P. S. Cuartielles, L. Felicetti, and S. Kemble, "Modified tisserand map exploration for preliminary multiple gravity assist trajectory design," 2020.

[28] B. Peherstorfer, K. Willcox, and M. Gunzburger, "Survey of multifidelity methods in uncertainty propagation, inference, and optimization," *Siam Review*, vol. 60, no. 3, pp. 550–591, 2018.

[29] M. A. Minovitch, "The invention that opened the solar system to exploration," *Planetary and Space Science*, vol. 58, no. 6, pp. 885–892, 2010.

[30] M. Lavagna, A. Povoleri, and A. Finzi, "Interplanetary mission design with aero-assisted manoeuvres multi-objective evolutive optimization," *Acta Astronautica*, vol. 57, no. 2-8, pp. 498–509, 2005.

[31] D. Izzo, "Advances in global optimisation for space trajectory design," in *Proceedings of the international symposium on space technology and science*, vol. 25, 2006, p. 563.

[32] M. Vasile, M. Ceriotti, V. M. Becerra, and S. Nasuto, "An incremental algorithm for the optimization of multiple gravity assist trajectories," in *Computational intelligence in aerospace sciences*. American Institute of Aeronautics and Astronautics, 2014, pp. 745–779.

[33] S. C. Shapiro, *Encyclopedia of artificial intelligence second edition*. John Wiley and Sons, Inc., 1987.

[34] C. M. Wilt, J. T. Thayer, and W. Ruml, "A comparison of greedy search algorithms," in *Third Annual Symposium on Combinatorial Search*, 2010, pp. 129–136.

[35] R. Eberhart and J. Kennedy, "A new optimizer using particle swarm theory," in *MHS'95. Proceedings of the Sixth International Symposium on Micro Machine and Human Science*. Ieee, 1995, pp. 39–43.

[36] J. Kennedy and R. Eberhart, "Particle swarm optimization," in *Proceedings of ICNN'95-international conference on neural networks*, vol. 4. IEEE, 1995, pp. 1942–1948.

[37] E. Ecale, F. Torelli, and I. Tanco, "Juice interplanetary operations design: drivers and challenges," in *2018 SpaceOps Conference*, 2018, p. 2493.

https://dspace.org/

A multi-fidelity optimization process for complex multiple gravity assist trajectory design

Bellome, Andrea; Sánchez Cuartielles, Joan Pau; Kemble, Stephen; Felicetti, Leonard

2021-06-25
ICATT
https://atpi.eventsair.com/QuickEventWebsitePortal/20a05-gnc-2020/website
Bellome A, Sanchez J-P, Kemble S, Felicetti L. (2021) A multi-fidelity optimization process for complex multiple gravity assist trajectory design. In: 8th International Conference on Astrodynamics Tools and Techniques, 23-25 June 2021, Virtual Event, The Netherlands

Downloaded from a DSpace repository. https://dspace.org/